Geological Society of America
Special Paper 369
2003

Carbon and oxygen isotope records from paleosols spanning the Paleocene-Eocene boundary, Bighorn Basin, Wyoming

Paul L. Koch*
Department of Earth Sciences, University of California, Santa Cruz, California, 95064, USA
William C. Clyde
Department of Earth Sciences, University of New Hampshire, Durham, New Hampshire 03824, USA
Robert P. Hepple
2380 Hilgard Avenue, Berkeley, California 94709, USA
Marilyn L. Fogel
Geophysical Laboratory, Carnegie Institute of Washington, Washington, D.C. 20015, USA
Scott L. Wing
Department of Paleobiology, Smithsonian Institution, Washington, D.C. 20560, USA
James C. Zachos
Department of Earth Sciences, University of California, Santa Cruz, California, 95064, USA

ABSTRACT

The isotopic composition of paleosol carbonate and organic matter were investigated in the Bighorn Basin, Wyoming, to explore changes in the carbon cycle and climate across the Paleocene-Eocene boundary. In three different measured sections, soil carbonate $\delta^{13}C$ values change in phase with marine surface water carbonates on both long (~7 m.y.) and short (~100 k.y.) time scales. The carbon cycle perturbations at the Paleocene-Eocene Boundary Thermal Maximum (PETM) and the Eocene Warm Interval (EWI) are recorded in multiple sections, providing unambiguous links between marine and continental deposits. The PETM and EWI $\delta^{13}C$ excursions in the Bighorn Basin are larger than those in the surface ocean, but the reasons for this amplification are unclear. Organic matter samples from the Bighorn Basin yield noisy $\delta^{13}C$ records that do not mirror global changes, perhaps due to diagenetic alteration or postformational contamination. The $\delta^{18}O$ values of soil carbonate are subject to multiple climatic influences that are often antagonistic. Although the $\delta^{18}O$ shifts at the PETM and EWI are small, the shift at the PETM is statistically significant in two of the measured sections. Assuming a plausible range of values for the meteoric water $\delta^{18}O$/mean annual temperature relationship, the perturbation in soil carbonate $\delta^{18}O$ at the PETM is consistent with an increase in meteoric water $\delta^{18}O$ of ~2‰ and changes in local temperature of 3–7 °C.

* pkoch@es.ucsc.edu

Koch, P.L., Clyde, W.C., Hepple, R.P., Fogel, M.L., Wing, S.L., and Zachos, J.C., 2003, Carbon and oxygen isotope records from paleosols spanning the Paleocene-Eocene boundary, Bighorn Basin, Wyoming, *in* Wing, S.L., Gingerich, P.D., Schmitz, B., and Thomas, E., eds., Causes and Consequences of Globally Warm Climates in the Early Paleogene: Boulder, Colorado, Geological Society of America Special Paper 369, p. 49–64.

INTRODUCTION

The Paleocene-Eocene (P-E) boundary is marked by biotic, climatic and environmental events that had a profound influence on Cenozoic Earth history. Oxygen isotope records from marine microfossils reveal a long-term warming of bottom waters and mid- to high-latitude surface waters spanning from ca. 59 to 50 million years ago (Ma) (reviewed in Zachos et al., 2001) (Fig. 1A). By the end of this long-term trend, global climates had reached a peak warming (referred to here as the Eocene Warm Interval [EWI]) that would not be surpassed for the rest of the Cenozoic. The $\delta^{13}C$ values of carbonates from ocean surface and deep waters dropped ~3.0‰ from the late Paleocene through the early Eocene, reflecting a long-term shift in the cycling of carbon among Earth surface carbon reservoirs (Fig. 1B). A brief (~150,000 year) pulse of extreme warming and a dramatic drop in $\delta^{13}C$ values were superimposed on these long-term trends near the P-E boundary (ca. 55 Ma) (Kennett and Stott, 1991; Röhl et al., 2000; Zachos et al., 2001). We will refer to this event as the Paleocene-Eocene Boundary Thermal Maximum (PETM). The short-lived drop in the $\delta^{13}C$ of marine carbonates at the PETM is best explained by the release and oxidation of at least 1500 gigatons of ^{13}C-depleted carbon from seafloor methane hydrate deposits, followed by sequestration of this excess carbon during carbon cycle reequilibration (Dickens et al., 1997; Dickens, 2000). The short-term warming at the PETM may reflect (in part) a greenhouse response to addition of this new carbon.

Events on land were no less profound. The most complete and best-studied terrestrial records spanning the P-E boundary occur in Wyoming. Physiognomic analyses of Wyoming floras indicate a long-term increase in mean annual temperature (MAT) of ~10 °C from the late Paleocene (Tiffanian [Ti] North American Land Mammal Age [NALMA]) to the late early Eocene (late Wasatchian NALMA), reaching temperatures of 20–25 °C (Wing, 1998; Wilf, 2000). Temperature increase was not monotonic, however. Isotopic data from fossil mammals and paleosol carbonates are consistent with short-term warming at the boundary between the Clarkforkian (Cf) and Wasatchian (Wa) NALMAs at 55 Ma (Koch et al., 1995; Fricke et al., 1998). Oxygen isotope records and floral analysis suggest that conditions subsequently cooled for perhaps 700,000 yr before warming renewed, reaching maximum values during the EWI in the late Wasatchian (Bao et al., 1999; Wing et al., 2000). There were significant faunal turnovers at the Ti-Cf and Cf-Wa boundaries at ca. 56.2 and 55 Ma, respectively (Gingerich, 1989; Clyde and Gingerich, 1998; Alroy et al., 2000), and a major floral turnover was associated with the EWI (Wing et al., 2000). Lastly, a sudden drop in the $\delta^{13}C$ of soil carbonates and mammal teeth in the northern Bighorn Basin (the Clarks Fork region) (Fig. 2) coincides precisely with the Cf-Wa boundary. This indicates that the earliest Wasatchian faunas (zone Wa 0), which contain the first primates, artiodactyls, and perissodactyls, were synchronous with the short-term warming and carbon cycle perturbation at the PETM (Koch et al., 1992; Bowen et al., 2001).

Here, we expand on prior isotopic work on Bighorn Basin paleosols (Koch et al., 1992, 1995), extending our records temporally to encompass middle-to-late Wasatchian paleosols, and geographically to incorporate data from sections in the McCullough Peaks region in the north-central Bighorn Basin and several regions in the southern Bighorn Basin. Carbon isotope analysis of paleosol carbonates and organic carbon sheds light on the timing of carbon cycle events on land and the response of continental carbon reservoirs to these events. Oxygen isotope analysis of paleosol carbonates serves as a monitor of climatically driven changes in the isotopic composition of meteoric precipitation and soil waters, as well as soil temperature. We end by synthesizing our new results with previous work on P-E climates in the Bighorn Basin.

CONTROLS ON CARBON AND OXYGEN ISOTOPES IN PALEOSOLS

The isotope systematics of soils and paleosols have been reviewed elsewhere (Cerling and Quade, 1993; Koch et al., 1995; Koch, 1998); these papers are the basis for our discussion. Soil carbonate carbon is derived from soil CO_2, which is supplied by decay of organic matter, soil respiration, and atmospheric CO_2. At depths >30 cm in even moderately productive soils, atmospheric inputs are negligible. The $\delta^{13}C$ of soil carbonate mirrors the isotopic composition of the overlying flora, offset by ~+15‰ due to fractionations associated with carbonate equilibria, diffusion of CO_2 from the soil, and decomposition/respiration.

The carbon isotope composition of plants is dependent on photosynthetic pathway (C3, C4 or CAM), environmental factors that influence photosynthetic rate (e.g., light intensity and water stress), and the $\delta^{13}C$ of atmospheric CO_2, the ultimate source of fixed plant carbon (Ehleringer and Monson, 1993). There is no compelling evidence that C4 or CAM plants were common in Paleogene floras (Jacobs et al., 1999). A recent meta-analysis of the carbon isotope fractionation between atmospheric CO_2 and C3 plants suggests that a difference of ~19‰ is to be expected under a range of conditions (Arens et al., 2000). Thus, the $\delta^{13}C$ of soil carbonates should roughly track changes in the $\delta^{13}C$ of atmospheric CO_2.

Finally, CO_2 in the atmosphere undergoes rapid exchange (tens of years) with the surface ocean, which in turn exchanges carbon with the massive deep ocean reservoir on longer time scales (hundreds to thousands of years) (Sundquist, 1993). At equilibrium, the difference in $\delta^{13}C$ between carbonate in the surface ocean and atmospheric CO_2 is ~9‰ (Mook, 1986), though the magnitude of this fractionation is affected by temperature and the $\delta^{13}C$ of local DIC can be affected by productivity. On geologic time scales, carbon exchange between the oceans and atmosphere is essentially instantaneous. Thus, shifts in the $\delta^{13}C$ of marine systems are transmitted via the atmosphere to terrestrial plants, soils, and mammals (Koch et al., 1992). Isotopic coupling of marine, atmospheric, and terrestrial carbon reservoirs is increasingly being used to correlate stratigraphic records

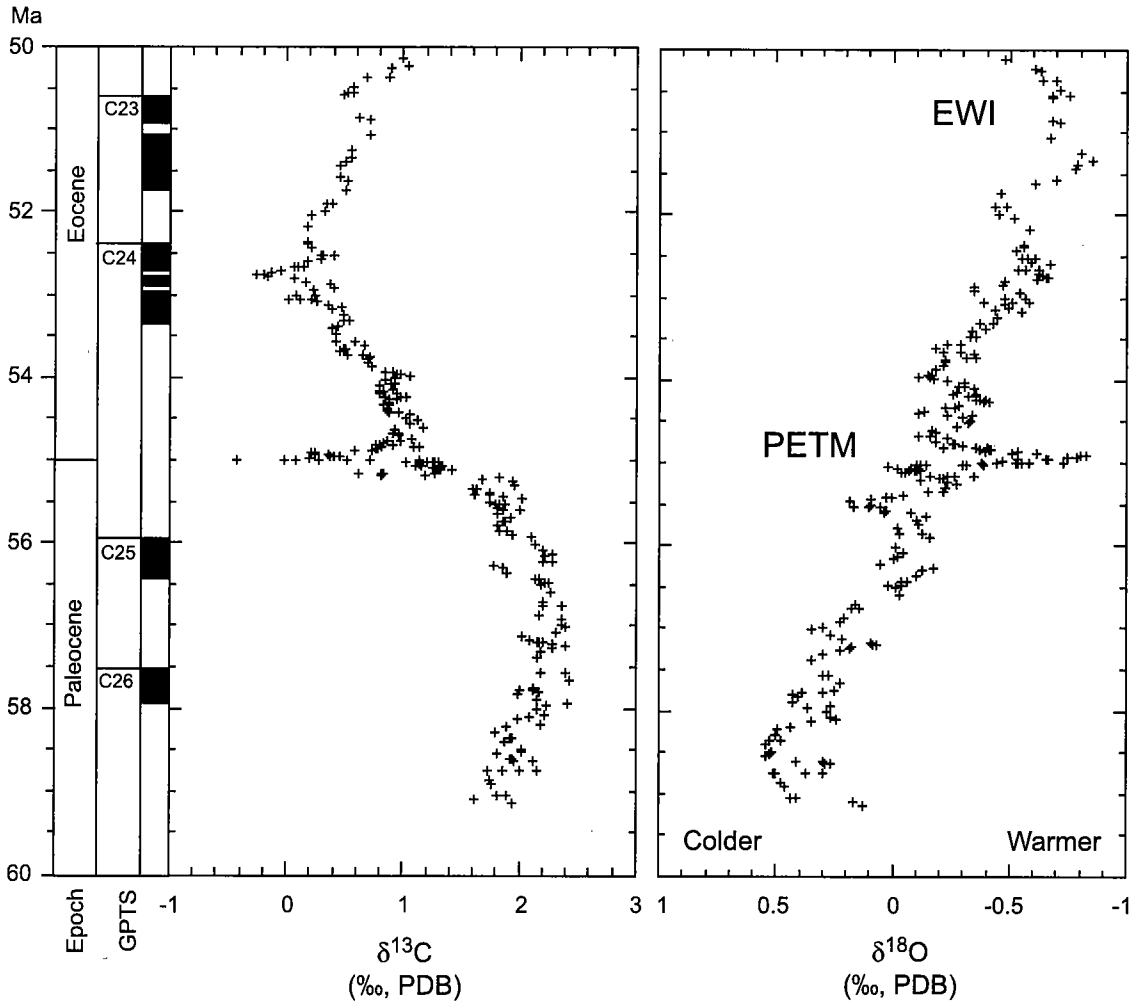

Figure 1. Carbon and oxygen isotope data for benthic foraminifera spanning the Paleocene-Eocene boundary. The figure is based on data compiled in Zachos et al. (2001). EWI—Eocene Warm Interval; GPTS—geomagnetic polarity time scale; PDB—Peedee belemnite; PETM—Paleocene-Eocene Thermal Maximum.

at times of global change, which are often marked by carbon cycle perturbations (MacLeod et al., 2000; Hesselbo et al., 2000; Jahren et al., 2001).

The oxygen isotope composition of soil carbonate is a function of the $\delta^{18}O$ of soil water and the temperature dependent fractionation of oxygen isotopes during carbonate formation. The $\delta^{18}O$ of modern, deeply formed soil carbonate is correlated with the $\delta^{18}O$ of meteoric water, though typically offset by 2‰–10‰ relative to equilibrium with meteoric water owing to evaporative enrichment of soil water. Shifts in the $\delta^{18}O$ of meteoric water, in turn, may be correlated to changes in atmospheric temperature (with lower $\delta^{18}O$ values at lower temperatures), or to changes in the source of water reaching a region. Overall, temporal changes in the $\delta^{18}O$ of soil carbonate may reflect the combined effects of several factors, precluding rigorous estimation of meteoric or climatic parameters. However, consideration of the potential magnitudes of these effects can provide some quantitative constraints on the magnitude of climatic perturbations.

MATERIALS AND METHODS

Authigenic carbonate nodules were sampled near the base of paleosol B-horizons from freshly trenched surfaces that had no evidence of modern soil development. Nodules were collected from at least 30 cm below the preserved top of the B horizon to minimize the influence of atmospheric CO_2 on $\delta^{13}C$ values and evaporation on $\delta^{18}O$ values. Plant fragment and cuticle samples were collected from fossil plant quarries or from organic-rich layers encountered during paleosol sampling. Blocks of organic-rich sediment were wrapped in aluminum foil to minimize contamination during transport.

Paleosol carbonate samples from the McCullough Peaks region were collected by W.C. Clyde during the course of paleo-

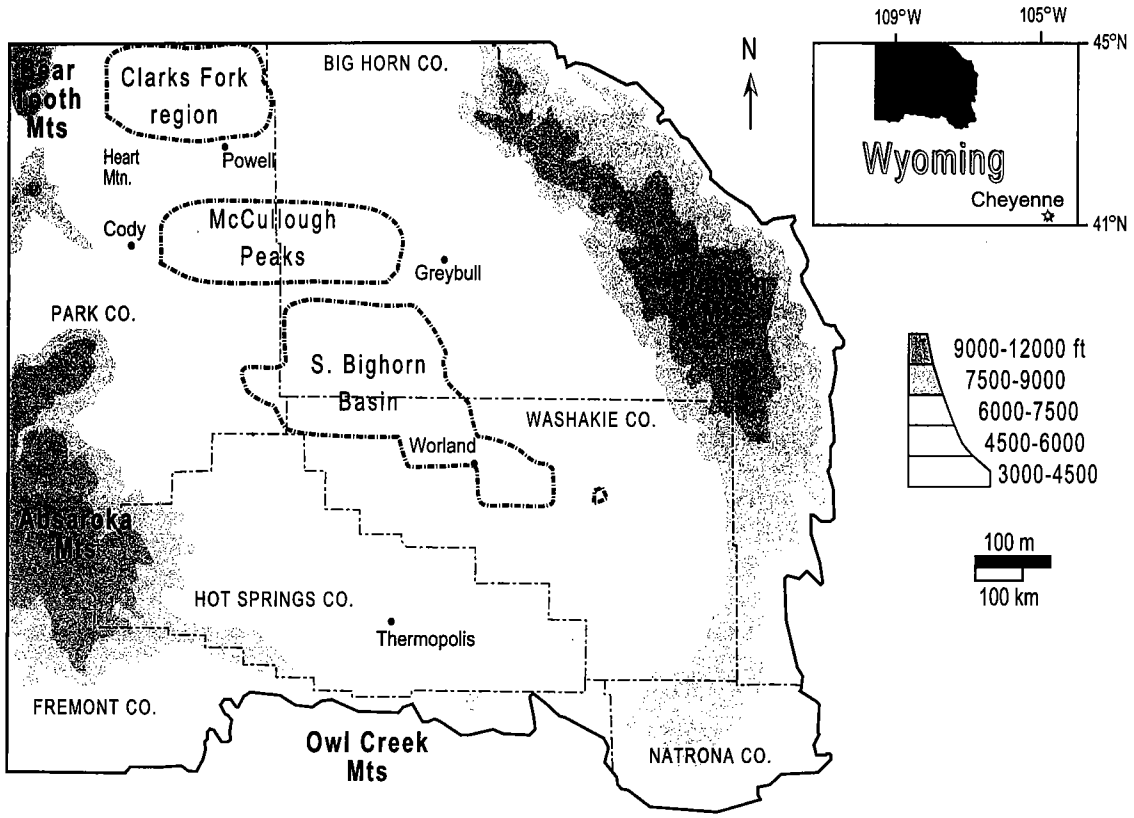

Figure 2. Map of the Bighorn Basin, Wyoming, showing the three regions of the basin where samples were collected from measured sections.

magnetic sampling. Samples are referenced by meter level relative to the Cretaceous-Tertiary boundary in the Southeast McCullough Peaks composite section (Clyde, 1997, 2001). Sediments below the Cf-Wa contact (~1195 m), which coincides with the Fort Union–Willwood Formation contact, do not contain paleosol carbonates.

Paleosol carbonate and organic matter samples in the southern Bighorn Basin were collected by P.L. Koch from fossil mammal or plant localities established by workers from Yale (YPM localities), Johns Hopkins/USGS-Denver (D localities), and the Smithsonian Institution (SLW and MBF localities), or from new measured sections (PK localities). Sampling localities were distributed among different subregions in the southern Bighorn Basin (Elk Creek/Antelope Creek, Fifteen Mile Creek, Worland East, North Butte) (Bown et al., 1994; Wing et al., 2000). Localities are referenced by meter level relative to the Cf-Wa boundary in the southern Bighorn Basin composite section (Bown et al., 1994). As in the McCullough Peaks region, sediments below the Cf-Wa boundary, which again coincides with the Fort Union–Willwood Formation contact, do not contain paleosol carbonates.

Organic matter samples from the Clarks Fork region were collected at localities established by workers from the Smithsonian (SLW and DCF localities), Yale (LJH localities) and the University of Michigan (SC localities). Localities in the Clarks Fork region are referenced by meter level relative to the Cretaceous-Tertiary boundary in the Clarks Fork Basin composite section (Butler et al., 1981). Paleosol carbonate data for the Clarks Fork region were reported in Koch et al. (1995). We have replotted those data here, substituting a subsample of data from a new, high-resolution record at the Cf-Wa boundary for the interval from 1480 to 1560 m (Bowen et al., 2001). Unlike the situation in the McCulloughs Peak and southern Bighorn Basin sections, the Fort Union–Willwood Formation occurs well below the Cf-Wa boundary (at 1070 m), and paleosol carbonates occur in the Fort Union formation into the Tiffanian NALMA.

Carbonate nodules were polished flat on a lapidary wheel, washed, and then dried in a low-temperature oven. Samples (~100 μg) were drilled from the polished surface under a binocular microscope using a mounted dental drill. Primary micritic carbonate and secondary diagenetic spar were sampled. When available, at least two micrite samples were drilled from each of two nodules from every soil that was sampled in the McCullough Peaks and southern Bighorn Basin sections. Samples were roasted in vacuo at 400 °C for 1 hr to remove organic contaminants and analyzed with a gas source mass spectrometer following reaction with 100% phosphoric acid at 90 °C using an automated Isocarb device. McCullough Peaks samples were an-

alyzed using the Optima mass spectrometer in the Department of Geological Sciences, Princeton University. Southern Bighorn Basin samples were analyzed using either the Optima or the Prism mass spectrometers in the Departments of Earth and Ocean Sciences, University of California, Santa Cruz. Carbonate isotope values are reported in delta notation relative to the V-PDB standard: $\delta = [(R_{SAMPLE}/R_{V\text{-}PDB}) - 1] \times 1000$, where R_{SAMPLE} and $R_{V\text{-}PDB}$ are the isotope ratios of the sample and standard, respectively. Analytical precision, based on repeated analysis of an in-house standard, was better than 0.1‰ for $\delta^{13}C$ and $\delta^{18}O$.

Two types of organic matter were analyzed. We analyzed fossil plant fragments and cuticles isolated from organic-rich rocks via digestion with HF. Samples were collected from fresh surfaces inside large blocks of lithified sediment. Plant fragments were stored in precombusted, teflon-lidded glass vials, whereas cuticle was suspended in alcohol. Cuticles were dried to volatilize alcohol prior to analysis. We also analyzed dispersed organic matter occluded within soil carbonate nodules. To extract this material, powdered paleosol carbonate was reacted with 1N HCl, then the insoluble residue was collected by centrifugation and rinsed repeatedly in distilled, deionized water. The residue was freeze-dried and stored in precombusted, teflon-lidded glass vials.

To obtain CO_2 for $\delta^{13}C$ analysis, organic samples were sealed in precombusted, evacuated quartz tubes with CuO and Cu metal, combusted at 900 °C for 1 hour, then cooled at a controlled rate. CO_2 was isolated cryogenically. CO_2 was analyzed on a Finnegan 252 at the Geophysical Lab or on the Optima at University of California, Santa Cruz. Repeated analyses of in-house gelatin standards prepared and analyzed in this manner had a standard deviation <0.15‰.

AGE MODEL

The Tiffanian and Clarkforkian NALMAs have been divided into numbered zones (e.g., Ti 1–6 and Cf 1–3) based on generic first occurrences and within lineage transformation events (Gingerich, 1983). Gingerich (1991) developed a numbered zonation of the Wasatchian based on first occurrences of perissodactyl species (supported by generic first occurrences in other orders [Gingerich, 2000]) that captured long-recognized concepts of the zones of the Wasatchian (Sandcouleean = Wa 0–2, Graybullian = Wa 3–5, Lysitean = Wa 6, Lostcabinian = Wa 7). This zonation was extended to the McCullough Peaks region by Clyde (1997, 2001). Unfortunately, zonation of the Wasatchian-aged sediments in the southern Bighorn Basin was last investigated in detail by Schankler (1980), and the perissodactyls from this region have not received systematic revision. Wa 0, Wa 5, 6, and 7 can be recognized in this region, but zones Wa 1–4 are grouped into Schankler's *Haplomylus-Ectocion* range zone.

Model ages for zone boundaries and tie points used to construct the age model are shown in Table 1. Calculation of an age model for the three sections follows Age Model 1 in Wing et al. (2000), incorporating revisions to the McCullough Peaks section presented in Clyde (1997, 2001). Briefly, reliable paleomagnetic data are available for the Clarks Fork and McCullough Peaks regions, but not for the southern Bighorn Basin. Yet, in the Clarks Fork region, the top of the section is unconstrained by magnetic reversals, whereas in the McCullough Peaks region, the base of the section lacks paleomagnetic constraints. We developed a hybrid model that incorporates estimates for the ages of two key events: The base of Wa 5 (*Bunophorus* Interval Zone) and the base of Wa 0, which coincides with the onset of the $\delta^{13}C$ excursion.

The logic of the model is as follows. Age estimates for magnetic reversals at the base and top of C24N.3n are used to calculate a sedimentation rate in the McCullough Peaks section that is then used to estimate an age for the base of Wa 5 by extrapolation. The age estimate for the base of Wa 5 is then used as a calibration point in the Clarks Fork Basin section. Assuming linear sedimentation between the top of C25N and the base of Wa 5, which are both present in the Clarks Fork Basin section, an age of 54.97 Ma is estimated for the base of Wa 0, which coincides with the $\delta^{13}C$ excursion. This age is then used as a calibration point at the base of the McCullough Peaks and the southern Bighorn Basin sections. Other calibration points are provided by age estimates for magnetic reversals in the Clarks Fork Basin and McCullough Peaks sections, and by an ash in the southern Bighorn Basin section (Table 1).

Although the age model has several potential sources of error, three lines of evidence suggest it is robust. First, the age estimate for the $\delta^{13}C$ excursion (54.97 Ma) is within the range (54.93–54.98 Ma) for the excursion in marine records, which was estimated via astronomical calibration (Norris and Röhl, 1999). Likewise, the age for the base of C24N.2n was not used to calibrate the age model, yet its estimated age in the McCullough Peaks section differs from the age reported in Cande and Kent (1995) by just 40,000 yr. Second, variations in sedimentation rate in the portions of the McCullough Peaks and Clarks Fork Basin sections that provide the calibration points are small (Table 1). Finally, age estimates for the bases of zones in different regions of the basin are similar. Differences between the Clarks Fork and McCullough Peaks regions are 0 and 170,000 yr for Wa 3 and Wa 4, respectively. Differences between McCullough Peaks and southern Bighorn Basin for the bases of Wa 6 and Wa 7 are larger (190,000 yr).

RESULTS

Data reliability was established in four ways. First, we collected multiple samples (from 2 to 4) from most nodules and calculated maximum within-nodule isotopic difference. The average maximum difference for McCullough Peaks nodules (n = 88) was 0.2‰ for both isotopes, whereas for southern Bighorn Basin nodules (n = 85), the average maximum difference for both isotopes was 0.4‰. Second, for most paleosols, we ana-

TABLE 1. AGE CALIBRATION

Event	Clarks Fork Basin Level (m)	Clarks Fork Basin Age (Ma)	McCullough Peaks Level (m)	McCullough Peaks Age (Ma)	Southern Bighorn Basin Level (m)	Southern Bighorn Basin Age (Ma)
Ash fall	N.A.	N.A.	N.A.	N.A.	**634**	**52.80**
Base of Wa 7 (*Lambdotherium* FAD)	N.A.	N.A.	2540	52.72	591	52.91
Top of C24N.2n	N.A.	N.A.	**2515**	**52.76**	N.A.	N.A.
Base of C24N.2n	N.A.	N.A.	2460	52.84	N.A.	N.A.
Top of C24N.3n	N.A.	N.A.	**2420**	**52.90**	N.A.	N.A.
Base of Wa 6 (*Heptodon* FAD)	N.A.	N.A.	2257	53.13	430	53.32
Base of C24N.3n	N.A.	N.A.	**2100**	**53.35**	N.A.	N.A.
Base of Wa 5 (*Bunophorus* FAD)	**2240**	**53.49**	2000	**53.49**	**365**	**53.49**
Base of Wa 4	2020	53.94	1665	54.11	N.A.	N.A.
Base of Wa 3 (*Homogalax* FAD)	1750	54.50	1450	54.50	N.A.	N.A.
Base of Wa 2	1645	54.72	1315	54.75	N.A.	N.A.
Base of Wa 1	1540	54.93	1205	54.96	N.A.	N.A.
Base of Wa 0	1520	**54.97**	**1195**	**54.97**	**0**	**54.97**
Base of Cf 3	1335	55.36	N.A.	N.A.	N.A.	N.A.
Base of Cf 2	1140	55.76	N.A.	N.A.	N.A.	N.A.
Top of C25N	**1070**	**55.90**	N.A.	N.A.	N.A.	N.A.
Base of Cf 1	935	56.17	N.A.	N.A.	N.A.	N.A.
Base of C25N	**820**	**56.39**	N.A.	N.A.	N.A.	N.A.
Base of Ti 6	815	56.41	N.A.	N.A.	N.A.	N.A.
Base of Ti 5	510	57.52	N.A.	N.A.	N.A.	N.A.
Top of C26N	**500**	**57.55**	N.A.	N.A.	N.A.	N.A.

Clarks Fork Basin Level (m)	Clarks Fork Basin Sed. rate (m/1000 yr)	McCullough Peaks Level (m)	McCullough Peaks Sed. rate (m/1000 yr)	Southern Bighorn Basin Level (m)	Southern Bighorn Basin Sed. rate (m/1000 yr)
2240–1070	0.48	2515–2420	0.65	634–365	0.39
1070–820	0.51	2420–2000	0.72	365–0	0.25
820–500	0.28	1195–2000	0.54		

Note: Level/age estimates in bold are the calibration points used for each composite section. Ages in bold that are underlined were determined in one section, then used as calibration points in the other two sections. Ages for all chron boundaries except the base of C24n.2n are from Cande and Kent (1995). N.A.—not applicable.

lyzed data from more than one nodule (up to 6). Using mean values for nodules (the average of all subsamples from the same nodule), we calculated the maximum within-soil difference for both isotopes. Within-soil differences in the McCullough Peaks soils (n = 41) were 0.5‰ and 0.4‰ for $\delta^{13}C$ and $\delta^{18}O$, respectively, whereas within-soil differences for southern Bighorn Basin soils (n = 40) were slightly higher (0.6‰ for both isotopes).

Third, in the southern Bighorn Basin, we analyzed sparry calcite in fractures to estimate isotopic values for the diagenetic end-member (GSA Data Repository Appendix 1[1]). In most cases, spar had much lower $\delta^{18}O$ values than micrite, indicating a higher temperature of formation. Spar $\delta^{13}C$ varied from values similar to those for micritic cements to very ^{13}C-depleted values. Thus, as in the study of the Clarks Fork region (Koch et al., 1995), contamination by diagenetic spar can be diagnosed by unusually negative $\delta^{18}O$ values, but the effect on $\delta^{13}C$ values is less pronounced.

Finally, soil development differs conspicuously among Bighorn Basin paleosols, and these variations might have an impact on isotope values from soil carbonates. In Data Repository Appendix 1, we report paleosol maturity values determined by Tom Bown for a subset of the southern Bighorn Basin paleosols. The maturity scale varies from stage 0 (least mature) to stage 5 (most mature) and can be modified to indicate whether soils are hydromorphic (Bown and Kraus, 1987). Increasing maturity, as indicated by increasing horizonation of the soil and increasing B horizon thickness, is thought to indicate increasing time of formation, though climate change (temperature, moisture) may affect the rate of soil maturation. The low density of maturity data prohibits quantitative analysis, but a cursory examination is informative. Samples from soils of similar maturity at adjacent stratigraphic levels (e.g., YPM 389 and YPM389 + 2 m, both stage 1 paleosols at 170 and 172 m, respectively) exhibit isotopic differences of the same magnitude as samples from soils of different maturity at adjacent levels (e.g., YPM 212 [stage 2H], YPM 290N [stage 1], and YPM 363 [stage 2] at 230, 210 and 190 m, respectively). Although the influence of soil maturity and hydromorphy certainly warrant further study, they impart no clear signal on the isotopic data reported here.

[1]GSA Data Repository item 2003048, Appendices 1–3, is available on request from Documents Secretary, GSA, P.O. Box 9140, Boulder, CO 80301-9140, USA, editing@geosociety.org, or at www.geosociety.org/pubs/ft2003.htm.

Mean $\delta^{13}C$ and $\delta^{18}O$ values for nodules are plotted versus stratigraphic level in Figures 3–5 along with 3-point running averages that illustrate trends. As reported in Koch et al. (1995), paleosol carbonate $\delta^{13}C$ values from the Clarks Fork region drop by ~3‰ from the late Paleocene (Ti 5/C25R) to the early Eocene (base of Wa 5) (Fig. 3). Superimposed on the long-term trend is a short-term drop of almost 8‰ to values as low as −16‰. Details of this excursion are explored in Bowen et al. (2001); we note here that the initiation of the excursion is nearly coincident with the first appearance of the three orders of modern mammals and the unusual Wa 0 fauna that marks the beginning of the Wasatchian NALMA. Oxygen isotope data show no long-term trends and typically range between −8‰ to −9‰. There is a suggestion that Wa 0 beds have less negative $\delta^{18}O$ values (Fig. 3). Nevertheless these higher values are balanced by adjacent low $\delta^{18}O$ values, so the running average does not show a significant deflection. ANOVA demonstrates that mean values for nodules are not significantly different between Wa 0 and beds below or above this zone.

The paleosol carbonate isotope record from the McCullough Peaks region begins with the Wa 0 beds and extends to the late Wasatchian (Wa 7) (Fig. 4; Data Repository Appendix

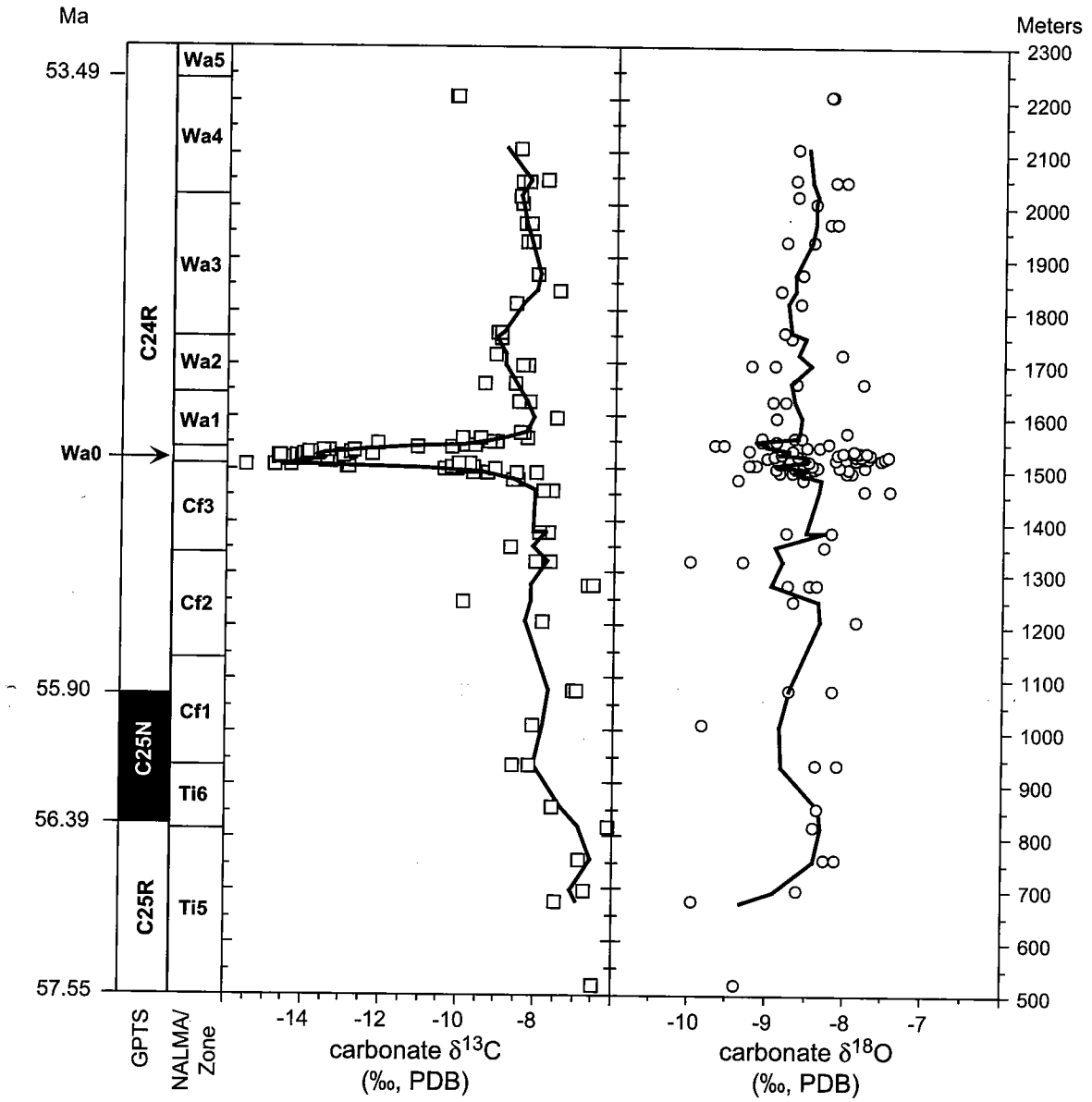

Figure 3. Carbon and oxygen isotope data for paleosol carbonates from the Clarks Fork region plotted versus meter level. The lines are 3-point running averages for meter-level mean values. Most data are from Koch et al. (1995), except for data near the Cf-Wa boundary, which are from Bowen et al. (2001). GPTS—geomagnetic polarity time scale; NALMA—North American Land Mammal Age; PDB—Peedee belemnite.

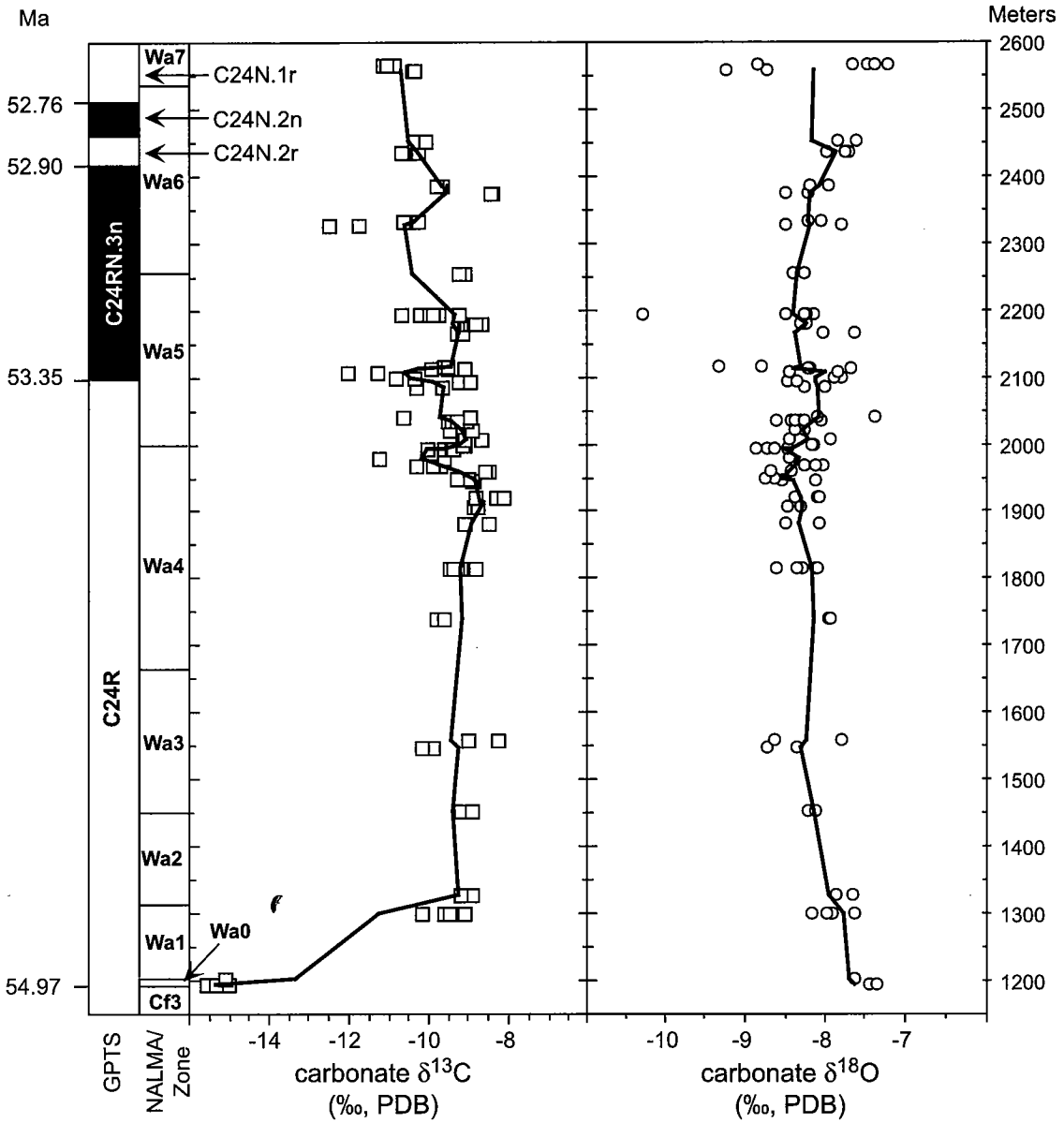

Figure 4. Carbon and oxygen isotope data for paleosol carbonates from the McCullough Peaks region plotted against meter level. Each data point represents the average of at least two analyses from each paleosol carbonate nodule. The lines are 3-point running averages for meter-level mean values. GPTS—geomagnetic polarity time scale; NALMA—North American Land Mammal Age; PDB—Peedee belemnite.

2; see footnote 1). The $\delta^{13}C$ record at the base of the section is similar to that in the Clarks Fork region. Wa 0 values are extremely low (~ –16‰), but values rise rapidly to –8‰ to –10‰ in Wa 1–4. $\delta^{13}C$ values show a second, more gradual decrease beginning in the middle of Wa 4, oscillating to a series of lows in Wa 5–6. The $\delta^{18}O$ record shows greater structure than in the Clarks Fork region. Wa 0 carbonates are consistently ^{18}O-enriched (mean nodule $\delta^{18}O$ value $\pm 1\sigma$: -7.6 ± 0.2‰, n = 4) relative to those from Wa 2–5 (-8.3 ± 0.4‰, n = 79). Values rise slightly in Wa 6–7 but show greater variability (-8.1 ± 0.5‰, n = 23). Differences in mean among these groups are significant (ANOVA, $p < 0.001$). Posthoc tests reveal that the Wa 0 to Wa 2–5 and Wa 2–5 to Wa 6–7 differences are significant; the difference between Wa 0 and Wa 6–7 is not (Scheffé's test).

The paleosol carbonate record from the southern Bighorn Basin also begins at Wa 0 and extends to Wa 7 (Fig. 5). $\delta^{13}C$ values for the Wa 0 beds are strongly negative, but not as ^{13}C-depleted as those from the other two sections. Following the rapid rise above the Wa 0 beds, values rise more gradually to the middle of the Upper *Haplomylus-Ectocion* zone (middle Wa

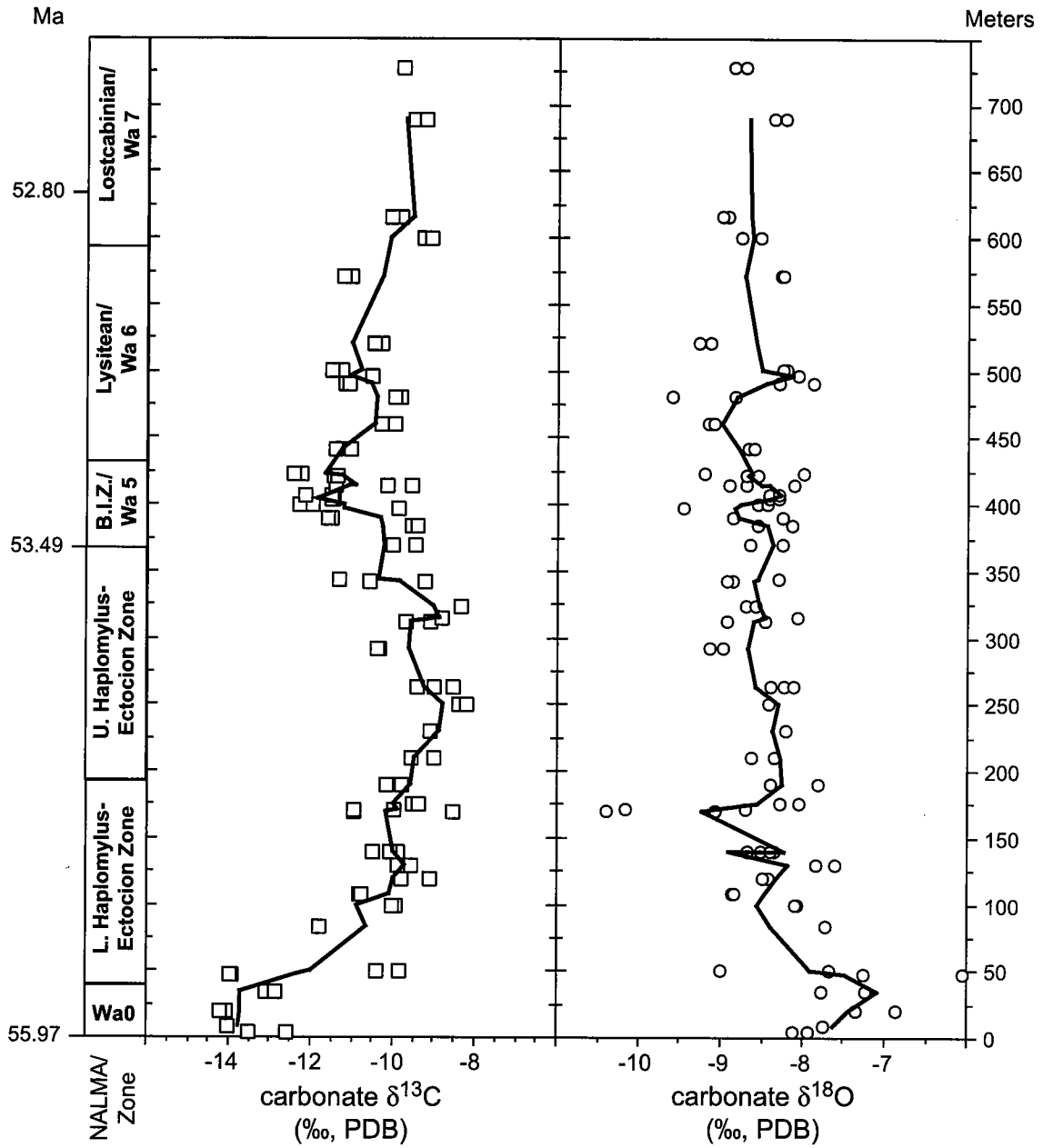

Figure 5. Carbon and oxygen isotope data for paleosol carbonates from the southern Bighorn Basin plotted against meter level. Each data point represents the average of at least two analyses from each paleosol carbonate nodule. The lines are 3-point running averages for meter-level mean values. NALMA—North American Land Mammal Age; PDB—Peedee belemnite.

4?), then drop gradually to a low in the *Bunophorus* Interval Zone (Wa 5). Values for the remainder of the section stay somewhat lower than the peak values in the *Haplomylus-Ectocion* zone. As in the McCullough Peaks section, carbonates from Wa 0 are consistently ^{18}O-enriched (–7.4 ± 0.6‰, n = 9) relative to samples from higher in the section (–8.6 ± 0.5‰, n = 84). This difference in mean is significant (t-test, $p < 0.0001$). Unlike the McCullough Peaks record, there is no return to higher $\delta^{18}O$ values in Wa 6–7.

Organic carbon records are plotted versus model age in Figure 6. Organic carbon within paleosol carbonates from the Clarks Fork region shows no change from the base of Ti 5 to the base of Wa 5. We sampled organics in carbonates from the Wa 0 beds intensively (SC 67 and SC 351, DR Appendix 3 [see footnote 1]). They show among the lowest values for the sequence (–25.3 ± 0.2‰ for Wa 0 soils vs. –24.8 ± 0.6‰ for the non-Wa 0 soils). This difference in mean is statistically significant (t-test, $p < 0.001$).

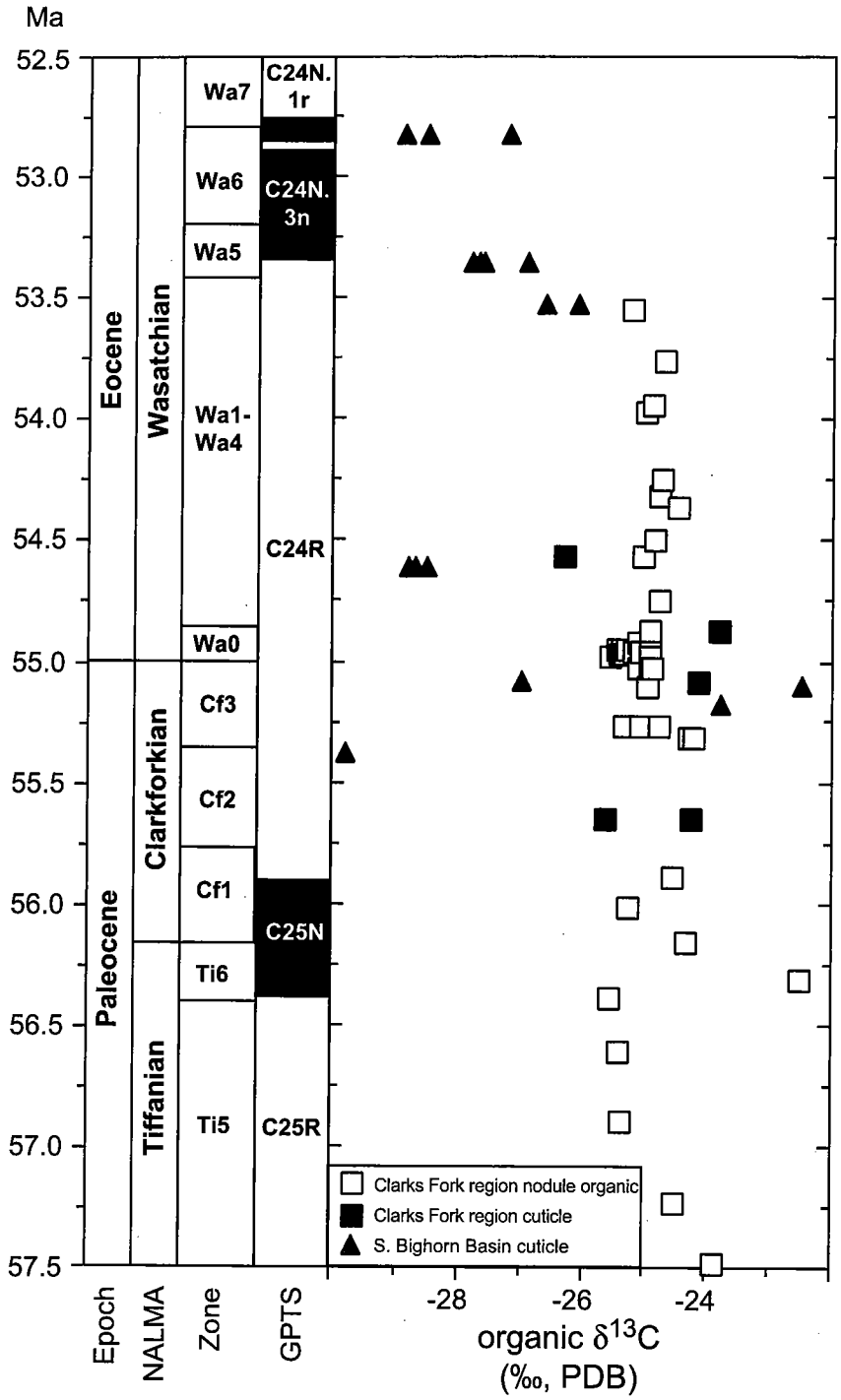

Figure 6. Carbon isotope data for cuticle and organic matter occluded in paleosol carbonates from the Bighorn Basin plotted against model age. GPTS—geomagnetic polarity time scale; NALMA—North American Land Mammal Age; PDB—Peedee belemnite.

Fossil cuticles and plant fragments from organic-rich beds are typically ^{13}C-depleted relative to nodule-occluded organic matter from adjacent horizons. In addition, cuticle and plant fragments from adjacent layers show a greater spread of values. We suspect that some of this variance is related to preservation. Well-preserved cuticle (pale brown with good cellular/morphologic preservation) typically has lower $\delta^{13}C$ values than poorly preserved samples (carbonized/black samples with poor morphologic preservation). This phenomenon merits further study, but at present, it limits the utility of plant fragments as a data source in our system.

DISCUSSION

Carbon isotopes: Correlation and the carbon cycle

If our conceptual model of the controls on soil carbonate $\delta^{13}C$ values is correct, then coeval carbonates from different

parts of the Bighorn Basin should have similar values, and secular trends on land should be of the same direction and roughly the same magnitude as those in marine surface waters. Both these issues are best viewed by combining soil carbonate $\delta^{13}C$ values from the different sections and plotting them relative to model age (Fig. 7). Where the three sections overlap in time (Wa 0–4), they show similar values, with two exceptions. First, in the southern Bighorn Basin, $\delta^{13}C$ values rise to postexcursion values over ~500,000 yr, whereas in the other two sections, the rise occurs in ~100,000 yr. This may reflect a problem with the assumption of constant sedimentation rate in the lower 365 m of the southern Bighorn Basin section, which underpins the age model. However the variations in sedimentation rate needed to bring the southern Bighorn Basin into accord with the other two records are large. Alternatively, we may be detecting differences in soil properties that affect isotope values (Cerling and Quade, 1993) or in the type of C3 vegetation overlying this region. The second difference is that Clarks Fork soil carbonates are consistently ^{13}C-enriched by 1‰–2‰ relative to those from the other two sections in the interval from 54.25 to 53.75 Ma. Again, this difference could relate to within-basin differences in soil properties or vegetation. For example, we might suspect that the

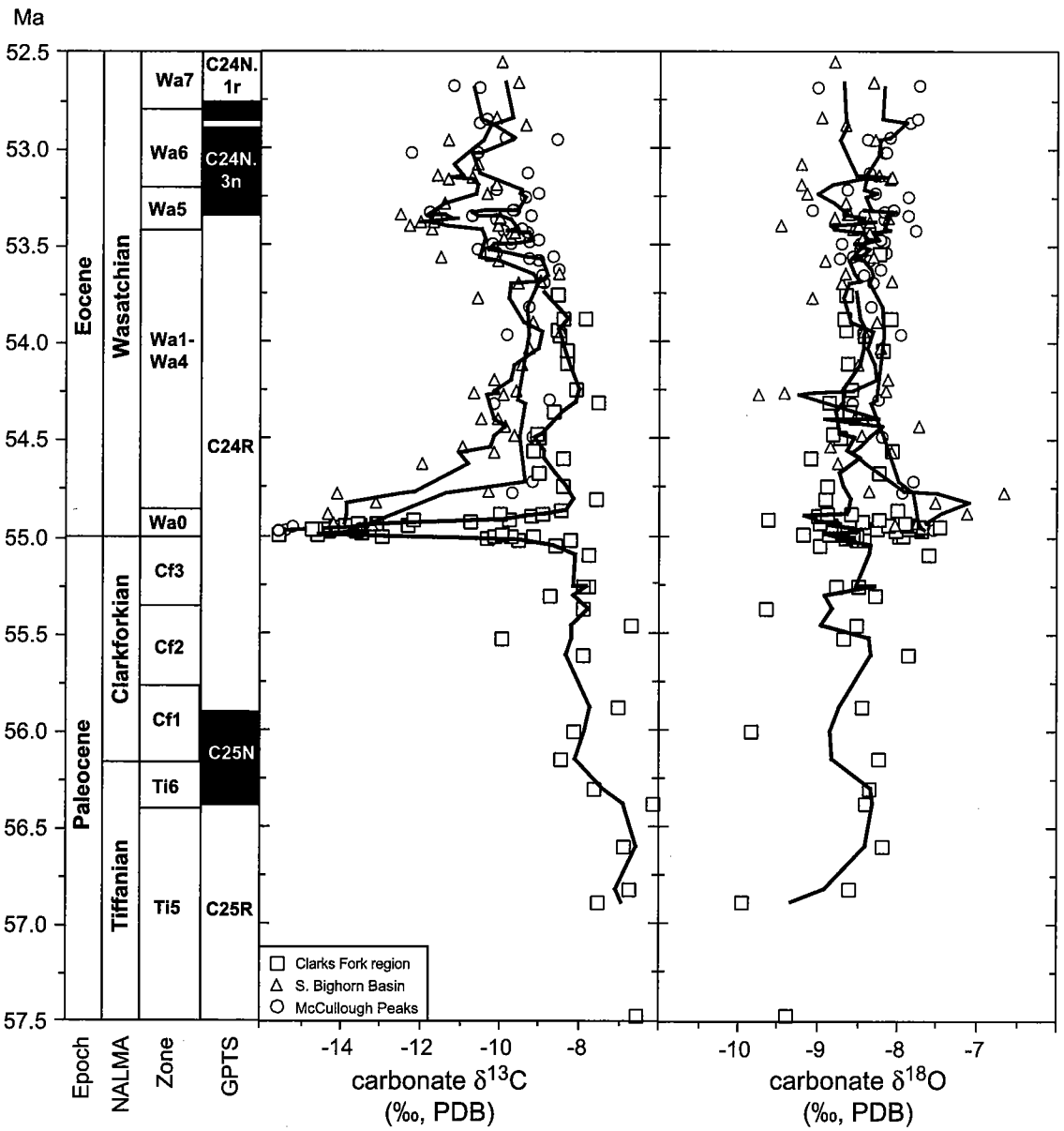

Figure 7. Carbon and oxygen isotope data for paleosol carbonates from three different regions within the Bighorn Basin plotted against model age. Each data point represents the average values of a particular meter level. In the southern Bighorn Basin and McCullough Peaks region, data from at least two different paleosol carbonate nodules were used to generate the level mean. The lines are 3-point running averages for each measured section. GPTS—geomagnetic polarity time scale; NALMA—North American Land Mammal Age; PDB—Peedee belemnite.

Clarks Fork region was drier than the rest of the Bighorn Basin during this interval, which would contribute to higher $\delta^{13}C$ values through lower soil productivity and water stress effects on plant isotope compositions (Cerling and Quade, 1993; Ehleringer and Monson, 1993). The higher incidence of hydromorphic soils and organic-rich shales in this interval in the southern Bighorn Basin is intriguing, but the issue clearly needs further, careful study.

Despite these small within-basin deviations, the long-term drop in $\delta^{13}C$ values on land matches the long-term marine shift well. Values on land drop by 4‰, from ~ –7‰ in C25R to values of ~ –11‰ in C24N.3n. Over this same temporal interval, values of marine surface and deep waters drop by ~2.5‰ (Fig. 1). Thus, the shift in continental records is of the same direction, but slightly magnified. There is a suggestion that $\delta^{13}C$ values begin to rise in C24N.2n, as they do in the marine record, but Bighorn Basin terrestrial sections are truncated by the cessation of paleosol formation.

Another intriguing feature of the Bighorn Basin $\delta^{13}C$ record relates to variability. The range in $\delta^{13}C$ values in Wa 5–7 (~4‰) is higher than the range in Wa 2–4 or in the Clarkforkian and Tiffanian (~2‰). Inspection reveals that increased variability is not solely a result of combining data from independent sections. The reason for increased variability is unclear, but it may relate to the rise in temperatures toward the EWI. Clyde et al. (2001) have recently reported highly variable paleosol carbon and oxygen isotope records from early Bridgerian-aged rocks (ca. 50 Ma) in the Green River Basin, Wyoming. These soils were formed during the EWI. Isotopic cycles in these soils seem to follow 100,000 year eccentricity cycles, suggesting that climatic forcing of vegetation change or the hydrologic cycle during this time of extreme global warming may be affecting soil formation processes. High-resolution (soil-by-soil) analysis of records from the top of the McCullough Peaks section, which has excellent paleomagnetic control, could reveal whether variability in this section is following Milankovich cycles, and it might point to the proximate link between isotopic variability and climate change.

The duration, direction, and time of onset of the short-term $\delta^{13}C$ excursion at the Cf-Wa boundary all demonstrate unambiguously that it is associated with the short-term carbon cycle perturbations at the PETM in marine systems. Still, the magnitude of the event on land (~8‰) is much greater than that in marine surface waters (2.5‰–4‰) (Kennett and Stott, 1991; Zachos et al., 2001). Potential causes for the amplified magnitude of the excursion on land are discussed in Bowen et al. (2001), but at present, the issue is unresolved. A second striking feature of the excursion on land is that its magnitude is reduced by ~2‰ in the southern Bighorn Basin relative to the other two sections. One possible explanation is that the Wa 0 beds in the southern Bighorn Basin do not record the onset of the excursion, where $\delta^{13}C$ values are lowest (Figs. 3–5). It is also possible that the base of Wa 0 is preserved in underlying Fort Union Formation lithologies where no pedogenic carbonate is preserved. The Fort Union–Willwood Formation contact is time transgressive in the northern part of the basin (e.g., the contact lies in the Clarkforkian NALMA in the Clarks Fork region but at the base of Wa 0 in the McCullough Peaks). This pattern may extend into the southern basin as well. Another possible explanation for the reduction in magnitude in the southern Bighorn Basin is time averaging. The Wa 0 paleosols in this area are among the most mature found anywhere in the basin. Maturity in part reflects the amount of time the original soil was exposed and active (Kraus and Bown, 1993). It is possible that Wa 0 paleosols in the southern Bighorn Basin have time averaged the $\delta^{13}C$ excursion more than the Wa 0 paleosols in the northern parts of the basin, where short-term accumulation rates are higher (and thus exposure times are shorter). Tests of these alternative explanations await development of better constraints on short-term sediment accumulation rates in these areas.

Plants are a key link in the chain connecting isotopic records from marine to atmospheric to continental carbon reservoirs. If sedimentary organic carbon records are derived from decayed ancient vegetation, they should show both the long-term and short-term shifts in $\delta^{13}C$ values. This prediction is not borne out by data from organic matter occluded in paleosol carbonates in the Bighorn Basin (Fig. 6). Nodule organic $\delta^{13}C$ values are invariant up-section, with a slight deflection toward lower values in Wa 0 soils. How can paleosol carbonates show a large decrease during this period of carbon cycle perturbation if soil organic matter does not? We can envision scenarios whereby soils receive a pulse of ^{12}C-enriched CO_2 directly from the atmosphere, perhaps via microbial oxidation of atmospheric methane. Yet this (and other) scenarios that explain the $\delta^{13}C$ excursion on land as a phenomenon restricted to soils are falsified by isotopic data from Bighorn Basin fossil mammals (Koch et al., 1995). Mammals obtain carbon only from plants, and they show an excursion as large as that seen in paleosol carbonates. We conclude that Paleocene-Eocene plants in the Bighorn Basin did show large $\delta^{13}C$ shifts in response to changes in the $\delta^{13}C$ of the atmosphere, but that these shifts are not recorded in the organic matter occluded in paleosol carbonates.

Paleosol nodules contain only trace amounts of organic matter. The most likely explanation for the invariant nodule organic data is that nearly all the original organic carbon has been removed by postburial oxidation. We are probably measuring traces of either modern Earth surface or basinal fluid organic carbon that is carried into nodules as a dissolved phase, and then sorbed to clay surfaces. Bird et al. (1994) demonstrated through stable isotope and ^{14}C analysis that even densely cemented pedogenic nodules are not closed with respect to organic carbon exchange, so the addition of trace amounts of organic carbon is not surprising. Values of –25‰ are within the range expected for degraded carbon from the contemporary C3 ecosystem that covers the land surface in Wyoming.

A clear implication is that great care must be taken when interpreting organic carbon records from organic-poor nodules. In the Paris Basin, Sinha et al. (1995) and Magioncalda et al.

(2001) studied bulk sediment organic matter, fragments of wood, and organic matter occluded within soil carbonate nodules. They detected a 6‰ drop in the $\delta^{13}C$ in "Sparnacian"-aged sediments that they correlated to the PETM. This result supports our contention that land plants exhibited a conspicuous $\delta^{13}C$ drop at the PETM. Clearly, the safest approach to constraining $\delta^{13}C$ shifts in plants is to use organic biomarkers characteristic of particular taxa, or at least to use clearly nontransported, ancient carbon sources such as well-preserved leaf cuticles or wood (e.g., Arens and Jahren, 2000; Hesselbo et al., 2000). Whenever possible, these records should be compared to associated carbon phases like soil carbonate or biogenic phosphate to evaluate potential diagenesis (as was done in the study by Sinha et al. [1995]).

Oxygen isotopes: Proxies for temperature and moisture

The clearest signal in the $\delta^{18}O$ records is at the PETM. In two of the three records (southern Bighorn Basin and McCullough Peaks), values are ^{18}O-enriched by at least 1‰ during the PETM. This enrichment in carbonate $\delta^{18}O$ values is consistent with several different scenarios.

The increase could reflect an increase in evaporative water loss from soils due to a decrease in regional precipitation. This scenario is not consistent with climate modeling results, which suggest an enhanced hydrological cycle during the PETM (Huber and Sloan, 1999). In addition, Wa 0 soils are extremely mature relative to soils higher or lower in the section. Increased maturity, which may reflect an increased intensity of chemical weathering, is more consistent with increased precipitation, higher temperatures, and greater soil productivity, not drier, less productive soils. Finally, this mechanism, which explains the shift in soil carbonate $\delta^{18}O$ values solely as a response to change in soil moisture ignores independent evidence that the $\delta^{18}O$ of meteoric water changed during the PETM. Oxygen isotope analysis of mammalian tooth enamel and gar scale ganoine suggest that meteoric water in the Bighorn Basin was ^{18}O-enriched by 2‰–3‰ during Wa 0 relative other intervals in the section (Fricke et al., 1998). In summary, we consider increased soil evaporation an unlikely source for the ^{18}O-enrichment in Wa 0/PETM soil carbonates.

An alternate explanation, which focuses on the shift in the $\delta^{18}O$ of Bighorn Basin meteoric water, is that the source of vapor masses supplying the region altered in response to the global climatic perturbations at the PETM. Today, precipitation reaching midcontinental North America that is derived from the Gulf of Mexico is ^{18}O-enriched relative to water arriving from the Pacific Ocean. Temporal shifts in vapor source region have been detected in $\delta^{18}O$ time series from Holocene and Pleistocene deposits (Amundson et al., 1996; Chamberlain and Poage, 2000). This difference is a result of the cooler temperatures of evaporation in the north-central Pacific (which cause vapor masses to be ^{18}O-depleted), and the strong rainout effects associated with transport over the mountains of the western United States. Although the altitude of the western United States in the Paleogene is a subject of controversy, it is very likely that altitudes to the west of Wyoming were greater than altitudes between Wyoming and Gulf of Mexico. We expect the same general pattern of difference in $\delta^{18}O$ values between Pacific and Gulf precipitation at the P-E boundary, though perhaps of lower magnitude. Thus, enhanced moisture supply from the Gulf of Mexico and Mississippi Embayment during the PETM could lead to ^{18}O-enrichment of meteoric waters and the soil minerals that form from them.

Another mechanism to change the $\delta^{18}O$ of meteoric water is to shift the seasonality of precipitation. Today, in regions where MAT is <20 °C, cool season precipitation is ^{18}O-depleted relative to warm season precipitation. In tropical regions, wet season precipitation is ^{18}O-depleted relative dry season precipitation. Thus, shifts in either the seasonality of rainfall or soil carbonate formation could contribute to ^{18}O-enrichment in the PETM.

None of the preceding scenarios entail a regional increase in temperature, which might be expected given the sharp global rise in ocean surface temperatures at the PETM (Huber and Sloan, 1999). Soil carbonate $\delta^{18}O$ values can serve as a very rough proxy for temperature, assuming that factors mentioned above are invariant. Temperature has antagonistic effects on the $\delta^{18}O$ of soil carbonates. In modern temperate and high-latitude regions, there is a strong positive correlation between the $\delta^{18}O$ of meteoric water and MAT, reflecting chiefly increased rainout of ^{18}O from vapor masses at lower temperatures (Dansgaard, 1964). In regions with a MAT between 0 and 20 °C, the slope for the spatial relationship between $\delta^{18}O$ of meteoric water and MAT is ~+0.6‰ per °C ($r > 0.8$) (Rozanski et al., 1993). The effect of temperature on the oxygen isotope fractionation between water and calcite is weaker and of the opposite sign; the slope for the relationship between the $\delta^{18}O$ of calcite and the temperature of formation is ~ –0.23‰ per °C (Friedman and O'Neil, 1977). We can add these effects to solve for the changes in temperature and meteoric water $\delta^{18}O$ value that are mutually consistent with the observed change in soil carbonate $\delta^{18}O$ values. Using this approach, the observed increase in soil carbonate $\delta^{18}O$ value of 1.25‰ is consistent with an increase in meteoric water $\delta^{18}O$ value of 2.0‰, and both are consistent with an increase in MAT of 3.4 °C (Table 2).

There has been considerable debate about the applicability of the spatially derived meteoric water $\delta^{18}O$/MAT relationship for reconstructing temporal shifts in MAT (Boyle, 1997; Jouzel et al., 1997). The meteoric water $\delta^{18}O$/MAT slope is sensitive to the pole-to-equator temperature gradient, as well as the temperature of evaporation. Although independent changes in these factors can produce complex results, we might expect that in a world with a shallower pole-to-equator temperature gradient, the slope of the relationship would be lower as well (Fricke and O'Neil, 1999). Table 2 evaluates the effects of assuming shallower slopes on the estimated changes in MAT and meteoric water $\delta^{18}O$ values. Using slopes ranging from +0.6‰ to +0.4‰ per °C, we estimate PETM changes in the meteoric water $\delta^{18}O$ values ranging from +2‰ to +3‰, consistent with estimates for

TABLE 2. ESTIMATING CHANGE IN MEAN ANNUAL TEMPERATURE AND METEORIC WATER $\delta^{18}O$ AT THE PETM FROM CHANGE IN SOIL CARBONATE $\delta^{18}O$

Meteoric water $\delta^{18}O$/MAT slope (‰, SMOW/°C)	Estimated soil calcite $\delta^{18}O$/MAT slope* (‰, SMOW/°C)	Estimated ΔMAT# (°C)	Estimated $\delta^{18}O_{meteoric\ water}$§ (‰, SMOW)
+0.6	+0.37	+3.4	+2.0
+0.5	+0.27	+4.6	+2.3
+0.4	+0.17	+7.4	+2.9

Notes: Δ—change in; MAT—mean annual temperature.

*Calculated by adding the temperature-dependent fractionation of oxygen isotopes between calcite and water (–0.23‰/°C) to the meteoric water/MAT slope.

#Calculated by dividing the shift in soil carbonate $\delta^{18}O$ (+1.25) by the value in column 2.

§Calculated by multiplying columns 1 and 3.

Bighorn Basin meteoric water from Fricke et al. (1998). The estimated rise in temperature ranges from 3.4 to 7.4 °C.

The lack of a conspicuous response in soil carbonate $\delta^{18}O$ values to the onset of the EWI is puzzling. Studies of leaf physiognomy suggest that MAT in the Bighorn Basin was ~4 °C higher at 52.5 Ma than it was at 54.5 Ma (Wing et al., 2000) and a similar rise in MAT has been detected in the nearby Green River Basin (Wilf, 2000). Oxygen isotope compositions of tooth enamel, gar scales, and iron oxides also seem to track the EWI warming (Fricke et al., 1998; Bao et al., 1999). Using the relationships presented in Table 2, we would expect soil carbonate $\delta^{18}O$ values to increase by +1.5‰ to +0.7‰. There is a suggestion of a greater number of ^{18}O-enriched values near the top of the McCullough Peaks section (Fig. 4) but the record is noisy, so there is no pronounced affect on the running average of $\delta^{18}O$ values.

The fact that the EWI warming seems to be clearly recorded in the $\delta^{18}O$ of mammalian enamel and fish ganoine but not in coeval soil carbonates is intriguing. Enamel and ganoine are characterized by small, tightly packed crystals of relatively insoluble carbonate hydroxylapatite, whereas soil carbonates are composed of more soluble micritic calcium carbonate. It is possible that the oxygen in enamel and ganoine is more resilient to diagenetic recrystallization than the oxygen in soil carbonates. Alternatively the lack of change in soil carbonates may be a real signal, indicating that the multiple controls on $\delta^{18}O$ have somehow acted in a compensatory fashion.

CONCLUSION

The simple conceptual model of carbon isotope coupling among oceanic, atmospheric, and terrestrial carbon reservoirs is supported by this study. Soil carbonate $\delta^{13}C$ values change in phase with marine surface water carbonates on both the long (~7 m.y.) and short (~100 k.y.) time scales. These shifts are much greater than average within-nodule and within-soil isotopic differences. The PETM isotopic excursion is present in long measured sections from three regions in the Bighorn Basin separated by ~100 km. In addition, the two new sections (McCullough Peaks, southern Bighorn Basin) provide the first evidence in the Bighorn Basin for the long-term $\delta^{13}C$ minimum in C24N. The long-term $\delta^{13}C$ trend in the Bighorn Basin closely matches a paleosol carbonate record from the Aix-en-Provence basin in France (Cojan et al., 2000), demonstrating the global nature of these carbon cycle perturbations. Interestingly, the PETM $\delta^{13}C$ excursion in the Bighorn Basin is much larger than that in surface ocean carbonates or in Aix-en-Provence, but the reason for this amplification is unclear and under investigation at present. Finally, organic substrates from the Bighorn Basin yielded noisy $\delta^{13}C$ records that did not mirror these global changes, perhaps due to variable alteration of cuticle fragments or postformational overprinting in organic-poor soil carbonates.

The $\delta^{18}O$ values of meteoric water and soil carbonate are influenced by multiple, antagonistic factors. The observed responses in $\delta^{18}O$ values at the PETM and EWI are small, scarcely greater than average within-soil $\delta^{18}O$ differences. Still, the $\delta^{18}O$ perturbation at the PETM is statistically significant in two of the measured sections. Assuming a range of plausible values for the relationship between meteoric water $\delta^{18}O$ and temperature, this perturbation is consistent with independent evidence for changes in meteoric water and changes in local temperature of 3–7 °C. Still, more robust measures of change in temperature and precipitation, such as those provided by leaf physiognomic analysis, will be required before the terrestrial climatic response at the PETM can be evaluated with confidence.

ACKNOWLEDGMENTS

We thank H. Bao, J. Gorman, M. Johnston, G. Kardon, A. Marr, and K. Rose for assistance in the field, and M. Hogan, B. Johnson, M. Toperoff, and K. Young for assistance in the laboratory. We thank D. Dettman, S. Hesselbo, and L. Stott for thoughtful reviews of the manuscript. Dana Royer supplied cuticle samples for analysis. This work would not have been possible without the decades of geological and paleontological research on the Bighorn Basin led by Tom Bown, Ken Rose and Phillip Gingerich, and their assistance throughout the course of this study is greatly appreciated. This research was supported by NSF

grants EAR 9105160 (to PLK, JCZ, and MLF) and EAR 9627953 (to PLK), and Princeton University.

REFERENCES CITED

Alroy, J., Koch, P.L., and Zachos, J.C., 2000, Global climate change and North American mammalian evolution: Paleobiology, v. 26 (supplement), p. 259–288.

Amundson, R., Chadwick, O., Kendall, C., Wang, Y., and DeNiro, M., 1996, Isotopic evidence for shifts in atmospheric circulation patterns during the late Quaternary in mid–North America: Geology, v. 24, p. 23–26.

Arens, N.C., and Jahren, A.H., 2000, Carbon isotope excursion in atmospheric CO_2 at the Cretaceous–Tertiary boundary: Evidence from terrestrial sediments: Palaios, v. 15, p. 314–322.

Arens, N.C., Jahren, A.H., and Amundson, R., 2000, Can C3 plants faithfully record the carbon isotopic composition of atmospheric carbon dioxide?: Paleobiology, v. 26, p. 137–164.

Bao, H., Koch, P.L., and Rumble, D., 1999, Paleocene-Eocene climatic variation in western North America: Evidence from the $\delta^{18}O$ of pedogenic hematite: Geological Society of America Bulletin, v. 111, p. 1405–1415.

Bird, M.I., Quade, J., Chivas, A.R., Fifield, L.K., Allan, G.L., and Head, M.J., 1994, The carbon isotope composition of organic matter occluded in iron nodules: Chemical Geology, v. 114, p. 269–279.

Bowen, G.J., Koch, P.L., Gingerich, P.D., Norris, R.D., Bains, S., and Corfield, R.M., 2001, A high-resolution isotope stratigraphy across the Paleocene–Eocene boundary at Polecat Bench, Wyoming: University of Michigan Papers on Paleontology, v. 33, p. 73–88.

Bown, T.M., and Kraus, M.J., 1987, Intergration of channel and flood-plain suites, I: Developmental sequence and lateral relations of alluvial paleosols: Journal of Sedimentary Petrology, v. 57, p. 587–601.

Bown, T.M., Rose, K.D., Simons, E.L., and Wing, S.L., 1994, Distribution and stratigraphic correlation of upper Paleocene and lower Eocene fossil mammal and plant localities of the Fort Union, Willwood, and Tatman formations, southern Bighorn Basin, Wyoming: U.S. Geological Survey Professional Paper 1540, p. 1–103.

Boyle, E.A., 1997, Cool tropical temperatures shift the global $\delta^{18}O$-T relationship: An explanation for the ice core $\delta^{18}O$-borehole thermometry conflict?: Geophyscial Research Letters, v. 24, p. 273–276.

Butler, R.F., Gingerich, P.D., and Lindsay, E.H., 1981, Magnetic polarity stratigraphy and biostratigraphy of Paleocene and lower Eocene continental deposits, Clarks Fork Basin, Wyoming: Journal of Geology, v. 89, p. 299–316.

Cande, S.C., and Kent, D.V., 1995, Revised calibration of the geomagnetic polarity timescale for the Late Cretaceous and Cenozoic: Journal of Geophysical Research ser. B, v. 100, p. 6093–6095.

Cerling, T.E., and Quade, J., 1993, Stable carbon and oxygen isotopes in soil carbonates, *in* Swart, P.K., et al., eds., Climate change in continental isotope records: American Geophysical Union Geophysical Monograph Series, v. 78, p. 344–345.

Chamberlain, C.P., and Poage, M.A., 2000, Reconstructing the paleotopography of mountain belts from the isotopic composition of authigenic minerals: Geology, v. 28, p. 115–118.

Clyde, W.C., 1997, Stratigraphy and mammalian paleontology of the McCullough Peaks, northern Bighorn Basin, Wyoming: Implications for biochronology, basin development, and community reorganization across the Paleocene–Eocene boundary [Ph.D. thesis]: Ann Arbor, University of Michigan, 271 p.

Clyde, W.C., 2001, Mammalian biostratigraphy of the McCullough Peaks area in the northern Bighorn Basin, Wyoming: University of Michigan Papers on Paleontology, v. 33, p. 109–126.

Clyde, W.C., and Gingerich, P.D., 1998, Mammalian community response to the latest Paleocene Thermal Maximum: An isotaphonomic study in the northern Bighorn Basin, Wyoming: Geology, v. 26, p. 1011–1014.

Clyde, W.C., Sheldon, N.D., Koch, P.L., Gunnell, G.P., and Bartels, W.S., 2001, Linking the Wasatchian–Bridgerian boundary to the Cenozoic Global Climate Optimum: New magnetostratigraphic and isotopic results from South Pass, Wyoming: Palaeogeography, Palaeoclimatology, Palaeoecology, v. 167, p. 175–199.

Cojan, I., Moreau, M.-G., and Stott, L.E., 2000, Stable carbon isotope stratigraphy of the Paleogene pedogenic series of southern France as a basis for continental-marine correlation: Geology, v. 28, p. 259–262.

Dansgaard, W., 1964, Stable isotopes in precipitation: Tellus, v. 16, p. 436–468.

Dickens, G.R., 2000, Methane oxidation during the late Paleocene Thermal Maximum: Bulletin de la Société Géologique de France, v. 171, p. 37–49.

Dickens, G.R., Castillo, M.M., and Walker, J.C.G., 1997, A blast of gas in the latest Paleocene: Simulating first-order effects of massive dissociation of oceanic methane hydrate: Geology, v. 25, p. 259–262.

Ehleringer, J.R., and Monson, R.K., 1993, Evolutionary and ecological aspects of photosynthetic pathway variation: Annual Review of Ecology and Systematics, v. 24, p. 411–439.

Fricke, H.C., and O'Neil, J.R., 1999, The correlation between $^{18}O/^{16}O$ ratios of meteoric water and surface temperature: Its use in investigating terrestrial climate change over geologic time: Earth and Planetary Science Letters, v. 170, p. 181–196.

Fricke, H.C., Clyde, W.C., O'Neil, J.R., and Gingerich, P.D., 1998, Evidence for rapid climate change in North America during the latest Paleocene thermal maximum: Oxygen isotope compositions of biogenic phosphate form the Bighorn Basin (Wyoming): Earth and Planetary Science Letters, v. 160, p. 193–208.

Friedman, I., and O'Neil, J.R., 1977, Compilation of stable isotope fractionation factors of geochemical interest: Data of Geochemistry. M. Fleischer. 440-KK: 1–12.

Gingerich, P.D., 1983, Paleocene–Eocene faunal zones and a preliminary analysis of Laramide structural deformation in the Clarks Fork Basin, Wyoming: Casper, Wyoming Geological Association, 34th Annual Field Conference, Guidebook, p. 185–195.

Gingerich, P.D., 1989, New earliest Wasatchian mammalian fauna from the Eocene of northwestern Wyoming: Composition and diversity in a rarely sampled, high–flood plain assemblage: University of Michigan Papers on Paleontology, v. 28, p. 1–97.

Gingerich, P.D., 1991, Systematics and evolution of early Eocene Perissodactyla (Mammalia) in the Clarks Fork Basin, Wyoming: Contributions from the Museum of Paleontology, University of Michigan, v. 28, p. 181–213.

Gingerich, P.D., 2000, Paleocene–Eocene boundary and continental vertebrate faunas of Europe and North America: GFF, v. 122, p. 57–59.

Hesselbo, S.P., Gröcke, D.R., Jenkyns, H.C., Bjerrum, C.J., Farrimond, P., Morgans-Bell, H.S., and Green, O.R., 2000, Massive dissociation of gas hydrate during a Jurassic oceanic anoxic event: Nature, v. 406, p. 392–395.

Huber, M., and Sloan, L.C., 1999, Warm climate transitions: A general circulation modeling study of the late Paleocene thermal maximum (similar to 56 Ma): Journal of Geophysical Research—Atmospheres, v. 104, p. 16633–16655.

Jacobs, B.F., Kingston, J.D., and Jacobs, L.L., 1999, The origin of grass-dominated ecosystems: Annals of the Missouri Botanical Garden, v. 86, p. 590–643.

Jahren, A.H., Arens, N.C., Sarmiento, G., Guerrero, J., and Amundson, R., 2001, Terrestrial record of methane hydrate dissociation in the Early Cretaceous: Geology, v. 29, p. 159–162.

Jouzel, J., Alley, R.B., Cuffey, K.M., Dansgaard, W., Grootes, P., Hoffmann, G., Johnsen, S.J., Koster, R.D., Peel, D., Shuman, C.A., Stievenard, M., Stuiver, M., and White, J., 1997, Validity of the temperature reconstruction from water isotopes in ice cores: Journal of Geophysical Research—Oceans, v. 102, p. 26471–26487.

Kennett, J.P., and Stott, L.D., 1991, Abrupt deep-sea warming, paleoceanographic changes, and benthic extinctions at the end of the Paleocene: Nature, v. 353, p. 225–229.

Koch, P.L., 1998, Isotopic reconstruction of past continental environments: Annual Review of Earth and Planetary Sciences, v. 26, p. 573–613.

Koch, P.L., Zachos, J.C., and Gingerich, P.D., 1992, Correlation between isotope records in marine and continental carbon reservoirs near the Paleocene–Eocene boundary: Nature, v. 358, p. 319–322.

Koch, P.L., Zachos, J.C., and Dettman, D.L., 1995, Stable isotope stratigraphy and paleoclimatology of the Paleogene Bighorn Basin (Wyoming, USA): Palaeogeography, Palaeoclimatology, Palaeoecology, v. 115, p. 61–89.

Kraus, M.J., and Bown, T.M., 1993, Short term sediment accumulation rates determined from Eocene alluvial paleosols: Geology, v. 21, p. 743–746.

MacLeod, K.G., Smith, R.M.H., Koch, P.L., and Ward, P.D., 2000, Timing of mammal-like reptile extinctions across the Permian–Triassic boundary in South Africa: Geology, v. 28, p. 227–230.

Magioncalda, R., Dupuis, C., Blamant, D., Fairon-Demaret, M., Perreau, M., Renard, M., Riveline, J., Roche, M., and Keppens, E., 2001, L'excursion isotopique du carbone organique ($\delta^{13}C_{org}$) dans les paléoenvironments continentaux de l'intervalle Paleocène–Eocène de Varangeville (Haute-Normandie): Bulletin de la Société Géologique de France, v. 172, p. 349–358.

Mook, W.G., 1986, ^{13}C in atmospheric CO_2: Netherlands Journal of Sea Research, v. 20, p. 211–223.

Norris, R.D., and Röhl, U., 1999, Carbon cycling and chronology of climate warming during the Paleocene–Eocene transition: Nature, v. 401, p. 775–778.

Röhl, U., Bralower, T.J., Norris, R.D., and Wefer, G., 2000, New chronology for the late Paleocene thermal maximum and its environmental implications: Geology, v. 28, p. 927–930.

Rozanski, K., Araguás-Araguás, L., and Gonfiantini, R., 1993, Isotopic patterns in modern global precipitation, *in* Swart, P.K., et al., eds., Climate change in continental isotope records: American Geophysical Union Geophysical Monograph Series, v. 78, p. 1–35.

Schankler, D.M., 1980, Early Cenozoic paleontology and stratigraphy in the Bighorn Basin, Wyoming: University of Michigan Papers on Paleontology, v. 24, p. 99–114.

Sinha, A., Aubry, M.-P., Stott, L.D., Thiry, M., and Berggren, W.A., 1995, Chemostratigraphy of the "lower" Sparnacian deposits (Argiles plastiques bariolées) of the Paris Basin: Israel Journal of Earth Sciences, v. 44, p. 223–237.

Sundquist, E.T., 1993, The global carbon dioxide budget: Science, v. 259, p. 934–941.

Wilf, P., 2000, Late Paleocene–early Eocene climate changes in southwestern Wyoming: Paleobotanical analysis: Geological Society of America Bulletin, v. 112, p. 292–307.

Wing, S.L., 1998, Late Paleocene–early Eocene floral and climatic change in the Bighorn Basin, Wyoming, *in* Aubry, M.-P., et al., eds., Late Paleocene–early Eocene climatic and biotic events in the marine and terrestrial records: New York, Columbia University Press, p. 380–400.

Wing, S.L., Bao, H., and Koch, P.L., 2000, An early Eocene cool period? Evidence for continental cooling during the warmest part of the Cenozoic, *in* Huber, B.T., et al., eds., Warm climates in Earth history: New York, Cambridge University Press, p. 197–237.

Zachos, J., Pagani, M., Sloan, L., Thomas, E., and Billups, K., 2001, Trends, rhythms, and aberrations in global climate 65 Ma to present: Science, v. 292, p. 686–693.

MANUSCRIPT ACCEPTED BY THE SOCIETY AUGUST 13, 2002

Printed in the USA